INVESTIGATIONS ON MICROSCOPIC CLEAVAGE FRACTURE STRESS

C. Jüde-Esser*, F. Grimpe* and W. Dahl*

Investigations were made with low carbon steel C 10 to study cleavage fracture occuring below and at general yield. The microscopic cleavage fracture stress $\sigma_f^* = \sigma_{yy}^{max}$ was determined using double-edge notched tensile (DENT) and four-point bend specimens (SENB4). The determination followed by 3D-FE calculations of our own or Griffiths and Owen (6). A significant influence of temperature on σ_f^* was found. It is discussed, whether this might be regarded as physically reasonable. The explanation is seen in terms of the thermal activation of dislocation movement, which is needed to produce the critical conditions for fracture.

INTRODUCTION

The original Orowan criterion (1) proposes that cleavage is induced when the maximum tensile stress below the notch root reaches a critical stress σ_f^*, which is nearly independent of temperature and strain rate (2). Previous investigations with DENT specimens yielded temperature dependent values for σ_{yy}^{max} (3,4). The influence of temperature was reduced by considering a characteristic distance x_c according to Ritchie et al (5). The aim of this study was to find out, whether the temperature dependence of σ_f^* is physically reasonable.

EXPERIMENTAL

A low carbon steel C 10 (TABLE 1) was chosen for the investigation. The ferrite grain size after heat treatment was determined to be ≈ 50 µm.
Specimen were machined according to FIGURE 1a and 1b. The notched tensile specimens were tested in the temperature range between 77K and 373K at three different crosshead speeds (TABLE 2). The four-point bend tests were performed between 77K and 253K. The procedure is given in FIGURE 2.

* Institute of Ferrous Metallurgy, Technical University Aachen, FRG

Finite Element Calculations. The maximum local tensile stress σ_{yy} is computed with the finite element program ABAQUS using the von Mises yield criterion and isotropic strain hardening. Isoparametric twenty-noded elements with reduced integration were employed for the 3D-calculations allowing for geometric non-linearities. The FE-calculations are load controlled. FIGURES 3a and 3b show the finite element model for the DENT-specimen and the SENB4-specimen respectively. The SENB4-tests were also analyzed using the standardized 2D-FE-calculations given in (6).

RESULTS AND DISCUSSION

The fracture and general yield stresses σ_f and σ_{gy} plotted as a function of temperature yield characteristic curves as shown in FIGURE 4 for series 1. The behaviour in the series 2 and 3 is similar. The transition temperatures T_{gy} and T_i are shifted to higher values with increasing crosshead speed (TABLE 2). The aimed expansion of the cleavage region to higher temperatures was achieved. So cleavage fracture was found in series 3 already at 253K.

The calculated σ_{yy}^{max}-values are shown together with the according lower yield stress-values in FIGURE 5. The results of the SENB-tests according to (6) and according to the 3D-FE calculation were plotted as a function of testing temperature together with the corresponding σ_{YS}-values in FIGURE 6. These results show a temperature dependence of the microscopic cleavage fracture stress for the tensile tests (at all crosshead speeds) as well as for the bending tests. It is also shown that there exists a nearly constant difference between σ_{yy}^{max} and σ_{YS}.

The present results are not conform with the generally acknowledged assumption that σ_f^* is a temperature independent material parameter. On the other hand, a temperature effect on σ_f^* has already been observed in several investigations (e.g.(7)). Thermal activation of cleavage fracture is imaginable in connection with dislocation movement. Considering that cleavage is always preceded by some amount of plasticity, it could be postulated that dislocation movement is an important part of the failure process (8).

In the following we want to show that the microscopic cleavage fracture stress σ_f^* is dependent on temperature by pointing out the qualitative coherence of σ_f^* and yield stress σ_{YS}.

According to FIGURES 5 and 6 the uniaxial yield stress is exceeded by an additional stress $\Delta\sigma$ before cleavage occurs. Therefore the Tresca - yield criterion which must be fulfilled requires:

$$\sigma_f^* - \Delta\sigma = \sigma_{YS} \quad \ldots\ldots\ldots\ldots\ldots\ldots\ldots\ldots (1)$$

The condition that the crack initiation takes place near the boundary of the plastic zone leads with the equations for the principal stresses

$$\sigma_1 = \sigma_{YS} + \sigma_3 \; ; \; \sigma_2 = \tfrac{1}{2} \cdot (\sigma_1 + \sigma_3) \; ; \; \sigma_3 = \Delta\sigma$$

and for the equivalent stress

$$\sigma_{eq} = \sigma_{YS}$$

to the following equation for the multi-axiality:

$$\sigma_m / \sigma_v = (\sigma_1 + \sigma_2 + \sigma_3) / (3 \cdot \sigma_{eq}) \; . \; (2)$$

$$\sigma_m / \sigma_v = \tfrac{1}{2} + \Delta\sigma / \sigma_{YS} \quad \ldots\ldots\ldots\ldots\ldots\ldots (3)$$

This equation shows that the ratio $\Delta\sigma/\sigma_{YS}$ is important for fracture. The calculated $\Delta\sigma/\sigma_{YS}$-values are given also in the FIGURES 5 and 6. From equation 1 (with eq. 3) it can be seen that the microscopic cleavage fracture stress σ_f^* is correlated with the relative stress triaxiality because of

$$\sigma_f^* = \sigma_{YS} \cdot (\tfrac{1}{2} + \sigma_m / \sigma_v) \quad \ldots\ldots\ldots\ldots\ldots\ldots (4)$$

Hence the microscopic cleavage fracture stress σ_f^* is dependent on the thermally activated lower yield stress. At lower temperatures cleavage occurs already at lower multi-axialities because of the decreasing relative multi-axiality with decreasing temperature (8). The temperature dependence of σ_f^* was also found for line-pipe steels with bainitic microstructures in (9).

CONCLUSIONS

The microscopic cleavage fracture stress is temperature dependent.
This dependence is due to the increase of the lower yield stress with decreasing temperature because of the necessary stress interval $\Delta\sigma$.
Therefore the quotient $\Delta\sigma/\sigma_{YS}$ has an important role.

ACKNOWLEDGEMENT

The authors gratefully acknowledge the financial support by the Deutsche Forschungsgemeinschaft (DFG).

REFERENCES

(1) Orowan, E.,
Rep. Prog. Phys. 12 (1948), pp. 185-232

(2) Knott, J.F.,
Proc. ECF 9 (1992), Vol. 2, pp. 1375-1400

(3) Kühne, K. and Dahl, W.,
Archiv Eisenhüttenwesen 54 (1983), pp. 439-444

(4) Dünnewald-Arfmann, H., Twickler, M., Twickler, R. and Dahl, W.,
Proc. ICF 7 (1989), Vol 1, pp. 231-238

(5) Ritchie, R.O., Knott, J.F. and Rice, J.R.,
J. Mech. Phys. Solids 21 (1973), pp. 395-410

(6) Griffiths,J.R. and Owen, D.R.J.,
J. Mech. Phys. Solids 19 (1971), pp. 419-431

(7) Curry, D.A.,
Metal Science 16 (1982), pp. 435-440

(8) Riedel, H. and Kochendörfer, A.,
Archiv Eisenhüttenwesen 50 (1979), pp. 173-178

(9) Dünnewald-Arfmann, H., Twickler, M., Twickler, R. and Dahl, W.,
Proc. ICSMA 8 (1988), Vol 2, pp. 1063-1070

C	Si	Mn	P	S	Al	Cu	Cr	Ni	V	N
.091	.190	.373	.027	.025	.003	.030	.045	.026	.010	.004

Table 1 Composition in wt-%

specimen	DENT			SENB4
series	1	2	3	4
crosshead speed, mm/s	0,0017	1,7	100	0,008
T_{gy}, K	123	160	173	153
T_i, K	173	193	253	-

Table 2 Transition temperatures

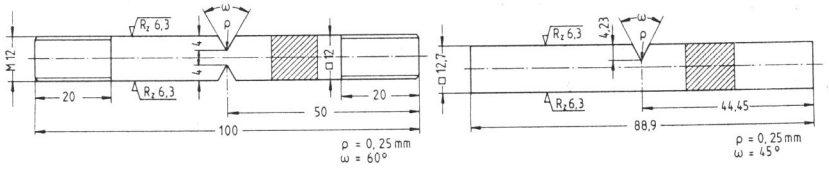

Figure 1 Specimen a) DENT b) SENB4

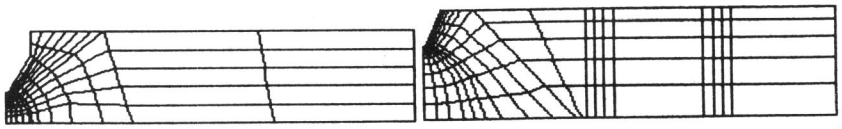

Figure 3 FE-meshes a) DENT b) SENB4

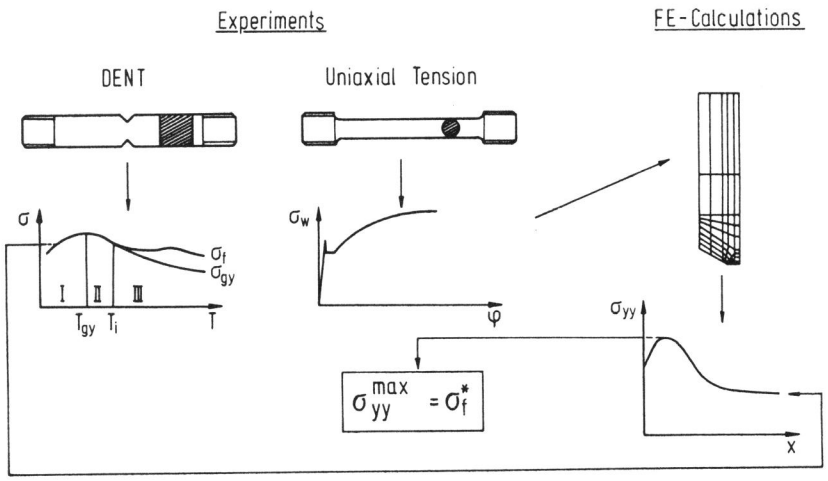

Figure 2 Determination of σ_f^*

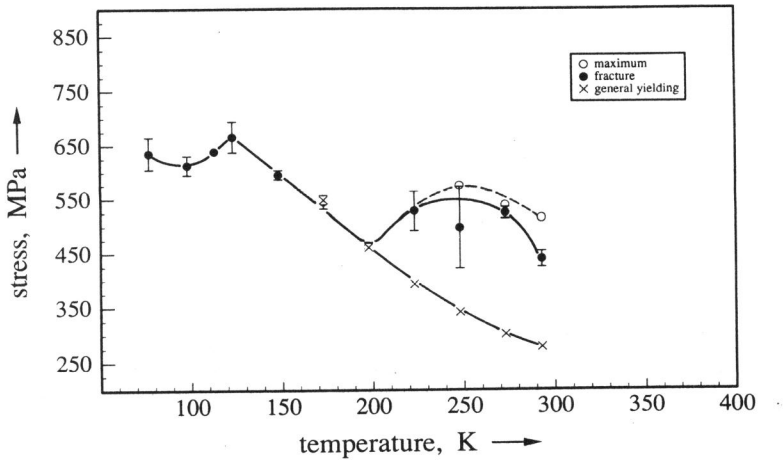

Figure 4 Graph of stress against temperature, series 1

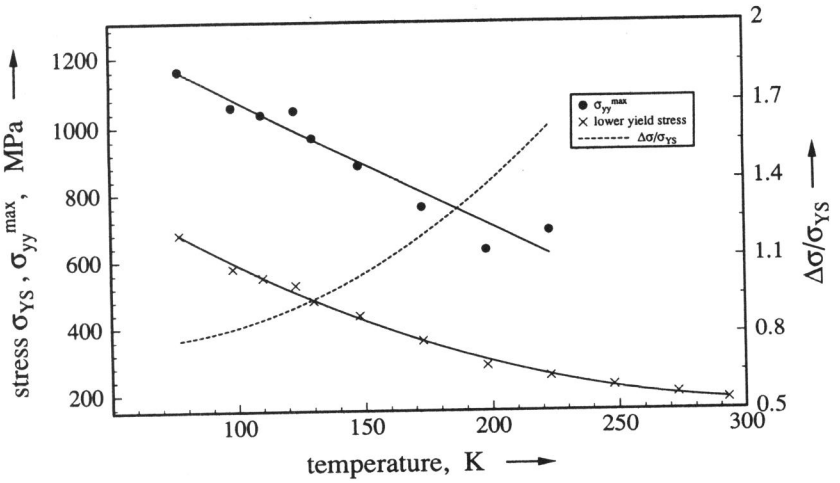

Figure 5 Graph of stress against temperature, series 1

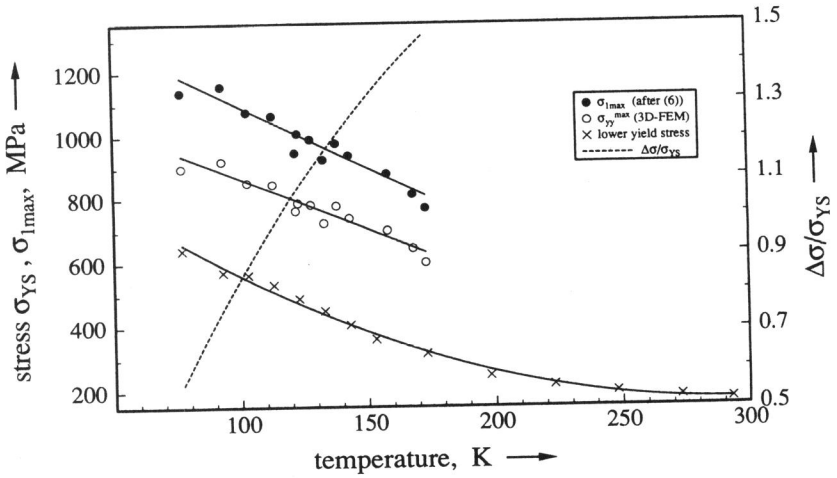

Figure 6 Graph of stress against temperature, series 4